ELSEVIER

Fuel 81 (2002) 431–448

FUEL

www.fuelfirst.com

Eastern Mediterranean sapropels: chemical structure, deposition and relation to oil-shales ☆

C. Dick[a], V. Ediger[b], D. Fabbri[c], A.F. Gaines[a,*], G.D. Love[d], A. McGinn[a], C. McRae[a], I.P. Murray[a], B.J. Nicol[a], C.E. Snape[a]

[a]*Department of Pure and Applied Chemistry, University of Strathclyde, Thomas Graham Building, 295 Cathedral Street, Glasgow G1 1XL, UK*
[b]*Institute of Marine Sciences, Middle East Technical University, P.O. Box 28, Erdemli 33731, Icel, Turkey*
[c]*Labortario di Chimica Ambientale, Dipartimento di Chimica 'G. Ciamician', Universita di Bologna, via Marconi 2, I-48100 Ravenna, Italy*
[d]*Institute of Fossil Fuels and Environmental Geochemistry, University of Newcastle, Drummond Building, Newcastle upon Tyne NE1 7RU, UK*

Received 12 May 2001; accepted 8 October 2001; available online 13 November 2001

Abstract

Ten sapropels, deposited in three different basins of the eastern Mediterranean since the Miocene and selected from cores of the Deep Sea Drilling Programme have been characterised by elemental analysis; fluorescence, infra-red and NMR spectrometry, by pyrolysis-gas chromatography/mass spectrometry and by catalytic hydrogenation at moderately high pressure. The sapropels are Types I–II kerogens, which have been oxidised, probably by a front experienced, since their deposition. Only one, from the Cretan basin, contained structures from lignin. The others, typical of a marine deposition, possessed aromaticities of about 0.2. Their detailed organic structures are described.

Keywords: Sapropels; Kerogen; Pyrolysis-gas chromatography/mass spectrometry; CPMAS NMR; Hy-Py

1. Introduction

1.1. Introduction: the samples

In a previous paper, Black Sea sapropels, whose deposition started about 5600 years ago, were shown to be impure alginites having a very similar organic structure to a Type I kerogen oil-shale [1]. We now extend the study of the organic structure of sapropels to include a range of 10 samples obtained from beneath the eastern Mediterranean by the Deep Sea Drilling Program (DSDP) [2]. Table 1 describes these samples, their labels and dating being those allocated by the DSDP, where descriptions of the geology and provenance of the samples can also be found [3–5].

1.2. Background: the deposition of the sapropels and their environment

At the beginning of the middle Miocene (about 14 million years ago), as a result of the anticlockwise rotation of the African Plate, the Tethys lost its function as an east–west seaway and became a semi-enclosed marginal Mediterranean basin [6,7]. Sapropel formation then occurred within the Mediterranean throughout the upper Miocene to the Quaternary in response to significant changes of climate, circulation and biogeochemical cycling [8–10]. Kidd et al.'s [3] definition of a sapropel as a 'discrete layer, greater than 1 cm in thickness, set in an open marine pelagic sediment and containing greater than 2% of organic carbon' was occasioned by the observation of several such layers in cores drilled from the eastern Mediterranean [2]. These Mediterranean sapropels contained assemblages of pollen and fossils, notably of foraminifers and orbulinas; dinoflagellates, diatoms and coccoliths [5], all testifying to the scenario that sapropel formation required a rich growth of vegetation,—either marine or terrigeneous—rapid deposition and subsequent preservation of the organic material, often under anoxic conditions [8,11]. There is continuing discussion of the relative contribution of these factors in the Mediterranean [11,12] and interested readers should pursue our selection of references.

The details of the upper Miocene deposition are not known to us, but sample 375/4-4 (Table 1) is an example of an upper Miocene sapropel. Subsequently, during the Messinean salinity crisis following the closure of what are now the Straits of Gibraltar, the Mediterranean twice

* Corresponding author. Tel.: +44-141-548-2282; fax: +44-141-548-4822.
E-mail address: a.f.gaines@strath.ac.uk (A.F. Gaines).
☆ Published first on the web via Fuelfirst.com—http://www.fuelfirst.com

0016-2361/02/$ - see front matter
PII: S0016-2361(01)00184-3

Table 1
The eastern Mediterranean sapropels [2–5]
(M: Miocene; P: Pliocene; Pl: Pleistocene; u: upper; and l: lower [3,4]) (L: label giving the location of the DSDP core and the position of the sample down the core [4,10]; BP: approximate time of deposition (millions of years before the present) [6]; *D* (m): depth of the sapropel sample below the sea bed (in metres) [3])

L	374/5-3	375/4-4	376/1-4	376/2-2	376/5-2	376/6-4	377/1-2	378/1-1	378/6-3	378/11-2
Basin	Ionian	Levant	Levant	Levant	Levant	Levant	Ionian	Cretan	Cretan	Cretan
Age	uP	M	uPl	Pl	Pl	P	Pl	Pl	P	P
BP	2.5	10	< 1	1	1	3	1	1	3	4
D (m)	300.5	250.5	5	10.5	38.6	50.5	191	85.3	144.8	304

evaporated [7]. Sapropels appear to have also been deposited during this time [8], when river water—and perhaps quantities of overflowing Atlantic water—accompanied by subsequent evaporation caused rapid deposition of organic sediments [9]. No such sapropels have been examined here.

Sapropels, such as those from cores 374, 376, 377 and 378 (Table 1) are a major characteristic of Pliocene and Quaternary sediments of the Mediterranean [15]. Paleoproductivity decreases from west to east and from the Pliocene to the Quaternary [15]. Lower Pliocene sapropels appear to have been deposited simultaneously over the whole basin, whereas the deposition of the upper Pliocene and Quaternary sapropels appears to vary with water-depth [15]. During the Pleistocene and Holocene, northern Africa appears to have been humid and regular monsoons caused flooding of a 'super-Nile' [6]. Sapropel depositions appear to have coincided with periods of maximum insolation and maximum flooding [6,10,16]. The flooding has been supposed to have generated a layer of less dense, brackish, nutrient-rich water in which phytoplankton bloomed on the surface of the eastern Mediterranean [6,15]. Convective mixing during the winters would have homogenised the sea thereby permitting settling of the phytoplankton to the bottom, possibly causing anoxia [15,17]. Indeed, it has been suggested [18–20] that diatomaceous mats, known to sink rapidly [18,19], formed in the surface layer and were deposited to yield sapropels. However, whereas the occurrence of diatoms has been observed in sapropels from the Aegean and Levantine basins, there is scant evidence of diatoms in sapropels from other basins, such as the Ionian [6] (samples 374/5-3 and 377/1-2) and other causes of sapropel deposition have been postulated [21]. The deposition of sapropels in the eastern Mediterranean terminated about 8000 years ago, when the present desertification of North Africa started and the monsoons ceased [22].

Thus, the deposition of sapropels ceased in the eastern Mediterranean, when the input of organic matter decreased and the bottom water became reventilated. Consequently, the redox regime changed from sulphidic to oxic, a downward oxidation front was initiated and migrated into the sediment forming a metal-rich zone above the sapropel [23]. In this way, the youngest sapropels deposited in the eastern Mediterranean appear to have experienced severe oxidative diagenesis, which has resulted in loss of some 60% of the original deposition of organic material [12, 23–29]. Accordingly, one should be extra cautious, when relating the chemical structures present in eastern Mediterranean sapropels to the structures in the original deposition.

1.3. Background: previous work

We know less about the geochemistry of sapropels from below the eastern Mediterranean than from below the Black Sea [1]. Deroo et al. [30], examined the bitumens from sapropels in cores 374, 375, 377 and 378 obtained by the DSDP and determined the hydrogen and oxygen to carbon ratios, the pyrolytic behaviour and the humic acid content of the kerogens. The results showed the kerogens to be scattered between Types II and III on a van Krevelen diagram. Ten Haven et al., determined $^{13}C-^{12}C$ ratios and analysed the lipids from Pleistocene [31,33] and Holocene [32,33] sapropels. Three sets of lipids were examined; free lipids obtained by extraction (bitumen), lipids obtained by saponification of the kerogen and lipids obtained by acid hydrolysis of the saponified kerogen; each set was characterised by gas chromatography/mass spectrometry (GC/MS). The $^{13}C:^{12}C$ ratios suggested the dominance of marine sources for the kerogens. In general, the compositions of the lipids obtained from most of these Quaternary sapropels were rather similar and showed them to contain organic material from both aquatic and terrigeneous vegetation, as well as from bacteria. The marine input was indicated by the observation of long chain unsaturated ketones (typical of those in the coccolithophore, *Emiliania huxleyi*), alkanediols, phytol, loliolide and many plant sterols. A lesser terrigeneous input was indicated by the distribution and the odd/even ratios of long chain alkanes, fatty acids and alkanols observed in the bitumen. A bacterial input was indicated by the observations of iso- and anteiso-fatty acids and of beta hydroxyacids after the acid hydrolysis of saponified kerogens. The composition of the lipids in Holocene sapropels obtained in the region of the Nile delta suggested a relatively larger input of aquatic vegetation and a relatively smaller input of terrigeneous vegetation than in Holocene sapropels obtained from cores from locations in the middle of the eastern Mediterranean [32]. This is consistent with the generation of the sapropels from a phytoplankton bloom

provoked by the flooding, nutrient-rich. Nile water, the bloom being less intense in the centre of the eastern Mediterranean since there, the nutrients from the Nile would have become diluted [32]. More recent work [27] appears consistent with these studies.

1.4. Aims

We report here characterisation of a set of 10 Miocene, Pliocene and Quaternary sapropels (Table 1) by elemental analysis, by infra-red, fluorescence and nuclear magnetic resonance (CPMAS NMR) spectrometry, by pyrolysis-gas chromatography/mass spectrometry (Py-GC/MS) and by high-pressure, catalysed hydrogenation (Hy-Py). The structure of the entire sapropel—rather than the small quantity of bitumen—is emphasised and compared to the structures of well-characterised kerogens, thereby giving the most complete characterisation of the organic material of the eastern Mediterranean sapropels known to us.

2. Experimental

2.1. Infra-red spectra

Fourier transform infra-red spectra were generated from potassium bromide discs by a Nicolet Impact 400D spectrometer.

2.2. NMR Spectra

^{13}C NMR spectra, using cross polarisation and magic angle spinning, CPMAS, were generated by a Brucker MSL 100 spectrometer from 250 mg of demineralised sapropels powdered to less than 250 μm diameter and packed into a 7 mm diameter zirconium tube with Kel-F caps. The tube and caps gave no background signal. Typically, 1000 scans were accumulated at 25 MHz using a contact time of 1 ms, a delay of 2 s between successive contacts and a pulse width of 3.6 μs. The ^{1}H decoupling and spin-locking field was 60 kHz and magic angle spinning was performed at 5 kHz. All spectra were processed using a line-broadening factor of 50 Hz.

2.3. Py-GC/MS

Pyrograms were obtained from a solution of about 5.5 mg/l of the internal standard (1,3,5-tri, *tert*-butyl benzene in methanol) placed in the centre of a quartz tube. Samples were pyrolysed at 700 °C for 10 s using the maximum heating rate of a CDS 1000 heated platinum filament pyroprobe. The pyrolysis products were swept into a Varian 3400 gas chromatograph, where they were separated by passing through a 30 m DB-5 fused silica capillary column (0.32 mm diameter and 0.25 μm film thickness) heated from 50 °C (held for 2 min) to 310 °C (held for 5 min) at 5 °C/min. The Py-GC interface and the injector (operating in the split mode) were maintained at 250 °C. The helium carrier gas travelled at 2 ml/min at 150 °C. The separated pyrolysis products were detected by a Varian Saturn II ion trap mass spectrometer employing 70 eV ionising electrons and conducting 1 scan a second over the mass range m/z 45–450. Identifications were based on comparisons with NIST 92, the Wiley data bank and previous workers' identifications of alkyl thiophenes [34], alkyl benzenes [35] and alkyl pyrroles [36]. The peak areas of the 46 compounds listed in Table 4 were determined in the SIM mode using the base and molecular ion peaks. Repeated quantitation of the peak area of the internal standard revealed a standard deviation of 10%.

2.4. Hy-Py

As described previously [37], 0.1–0.8 g of dry sapropel intimately mixed with 3% of ammonium dioxydithiomolybdate and diluted fivefold in fine, clean sand was plugged into a stainless steel tube and heated from 150 to 530 °C at 8 °C a minute in a hydrogen pressure of 15 MPa. Products collected in a trap cooled in solid carbon dioxide were dissolved in dichloromethane and separated into aliphatic, aromatic and polar fractions by column chromatography [37]. One microlitre samples of the aliphatic fractions were injected from a HP 7673 autosampler into a fused silica, capillary, CHP-5 column having a length of 25 m and a diameter of 0.25 mm and an internal surface coated with 95/5% methyl/phenyl silicone. Whilst, the samples were carried through the column by a 1 ml/min flow of helium, the column was heated from 170 to 225 °C at 6 °C/min and then to 300 °C at 4 °C/min; this temperature was maintained for 20 min. In this way, the samples were separated within a HP 5896 II gas chromatograph. Compounds leaving the column were characterised by an HP 5972 quadrupole mass selective detector (ionisation by 70 eV electrons; interface temperature 300 °C, source temperature 160 °C) and identified by comparison of their retention times and mass spectra with those of known standards and spectra recorded in the literature.

2.5. Fluorescence

Spectra of dilute suspensions of powdered, demineralised sapropels in distilled water and of dichloromethane-soluble bitumens were obtained from a Perkin–Elmer MPF44 Spectrofluorometer. Demineralised sapropels were carefully powdered in a pestle and mortar, mixed with excess distilled water and sonicated (for not more than 30 s at a time), the routine being repeated until a stable suspension was obtained.

3. Results

3.1. Infra-red spectra

All the infra-red spectra from the eastern Mediterranean

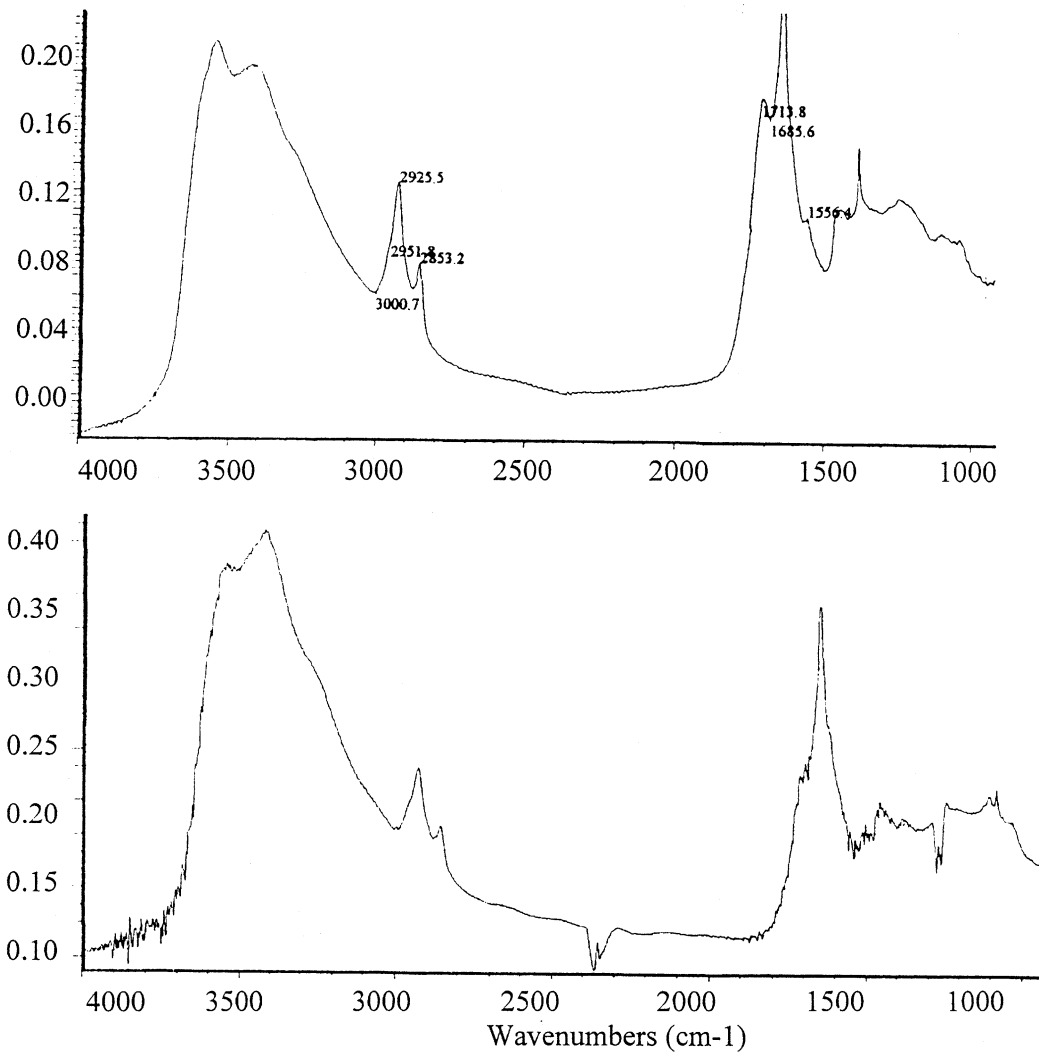

Fig. 1. Infra-red spectra of sapropels 376/2-2 (top) and 378/1-1 (bottom).

sapropels were similar in possessing absorption due to hydrogen bonded OH stretching vibrations (broad), aliphatic CH bending vibrations, the deformation vibrations of methyl groups and by carbonyl stretching vibrations (Fig. 1).

The similar sapropel spectra in the 1500–1750 cm^{-1} region differed from the spectra of kerogens. All sapropels displayed significant, spiky absorption at 1640–1650 cm^{-1} together with lesser, but resolved absorption at 1705–1715 cm^{-1} (Fig. 1). Sample 378/1-1, alone of the sapropels examined, also showed a shoulder of absorption at 1600 cm^{-1}, probably due to the vibrations of aromatic rings (Fig. 1). Treatment of the sapropels with zinc and hydrochloric acid reduced the absorption at 1640–1650 cm^{-1} and produced broad absorption around 1400 cm^{-1}. Seemingly, at least part of the absorption at 1640–1650 cm^{-1} was due to stretching vibrations of carbonyl groups associated with aromatic rings [38]. Washing of the sapropels with dilute potassium hydroxide replaced the absorption at 1705–1715 cm^{-1} by dual absorption at around 1635 and 1565–1570 cm^{-1}, consistent with the original 1705–1715 cm^{-1} absorption having been due to carbonyl vibrations in the carboxyl groups of aliphatic acids, which became carboxylate anions, when washed with potassium hydroxide [38]. No absorption due to the stretching vibrations of carbonyl groups in ester linkages was observed in any of the sapropels.

The presence of the 1640–1650 cm^{-1} absorption in the eastern Mediterranean sapropels and its absence in oil-shale and coal samples, we examined suggests the corresponding carbonyl groups to have been formed by the oxidation of methylene bridges or groups α to aromatic rings in the structure of the sapropel during the passage of an oxidation front after the sapropels had been deposited [12,23–29] or possibly during the rather prolonged storage of the sapropels. Should oxidation have occurred during the passage of a front, our results, consistent with those of workers examining samples obtained more recently

Table 2
Summarised ^{13}C CPMAS NMR spectra
(378/1-1*: results of two samples demineralised separately; BSS: Black Sea sapropel [1]; K1: Type I kerogen oil-shale [13]; K2: Type II kerogen oil-shale [14]; O/C and H/C: elemental ratios estimated from ^{13}C CPMAS NMR spectra; H/C*: elemental ratios determined directly on demineralised samples; f_a: fraction of carbon atoms, which were aromatic, determined from ^{13}C CPMAS NMR spectra; C_{ar}–O, C_{ar}–C and C_{ar}–H: aromatic carbon atoms combined with oxygen, carbon and hydrogen atoms, respectively; the numbers have been scaled so that the total number of aromatic carbon atoms is six, the number in a benzene ring; ($CH_2 \pm CH$)/ end CH_3: the ratio of the number of aliphatic carbon atoms in the range 15–45 ppm to the number in the range 0–15 ppm; this is the approximate average number of aliphatic carbon atoms per terminal methyl group; CH_2/CH_3^*: ratio of the infra-red absorptions due to the asymmetric stretching vibrations of methylene and methyl groups in the sapropels)

Sample	378/1-1*	376/6-4	376/5-2	376/2-2	375/4-4	BSS	K1	K2
O/C	0.35, 0.31	0.30	0.25	0.19	0.21	0.18–0.18	0.16	0.07–0.10
H/C	1.45, 1.30	1.79	1.87	1.71	1.78	1.79–1.72	1.70	1.24–1.44
H/C*	1.4	1.87	2.08	1.61	1.93		1.52	
f_a	0.40, 0.49	0.20	0.20	0.28	0.22	0.20–0.25	0.22	0.66–0.40
C_{ar}–O	1.69, 1.80	1.40	0.88	0.93	0.87	0.91–1.08	0.99	0.51–1.01
C_{ar}–C	1.01, 1.23	1.60	1.23	1.04	1.26	0.44–0.77	0.69	1.52–1.25
C_{ar}–H	3.30, 2.97	3.0	3.88	4.04	3.87	4.65–4.12	4.32	3.98–3.75
($CH_2 \pm CH$)/ end CH_3	5.75	3.9	4.3	3.25	7.85	11.6–10.7	8.1	2.9–5.9
CH_2/CH_3^*	2.5	2.7	2.3	2.0	3.6		3.8	1.8

[12,23–29], indicate this to have been a rather general phenomenon, not restricted to the latest sapropels to have been deposited in the eastern Mediterranean.

Ratios of the absorption due to the asymmetric stretching vibrations of methylene and methyl groups in the sapropels are included in Table 2.

3.2. NMR Spectra

All the demineralised sapropels examined save that of 378/1-1 gave qualitatively similar ^{13}C CPMAS NMR spectra, a typical example being shown in Fig. 2. Consistent with the infra-red spectra of these sapropels, their NMR spectra showed resolved absorption by carbon atoms

- in carbonyl groups (chemical shifts from 210 to 200 ppm),
- in carboxyl groups (chemical shifts from 185 to 170 ppm),
- attached to alcohols or aliphatic ethers (chemical shifts from 85 to 55 ppm),
- in methoxyl groups (chemical shifts near 55 ppm) and
- in aliphatic hydrocarbons (chemical shifts from 45 to 0 ppm including methines near 40 ppm, methylene groups γ and further from the ends of aliphatic chains near 30 ppm, methylene groups α to aromatic rings near 25 ppm, methyl groups α to aromatic rings near 20 ppm and methyl groups terminating alkyl chains from 15 to 0 ppm though, unfortunately, it was not possible to resolve each of these assignments on every spectrum).

In addition, absorption by carbon atoms in aromatic rings, including carbon atoms attached to oxygen, carbon and hydrogen atoms, was clearly observed between chemical shifts of 155 and 105 ppm. Fig. 2 also shows the unique spectrum given by demineralised samples of 378/1-1. This Pleistocene sample from the Cretan basin gave a structured spectrum with twice the absorption by aromatic carbon atoms shown by any of the other sapropels. Table 2 compares the NMR spectra using integrations of the various absorptions.

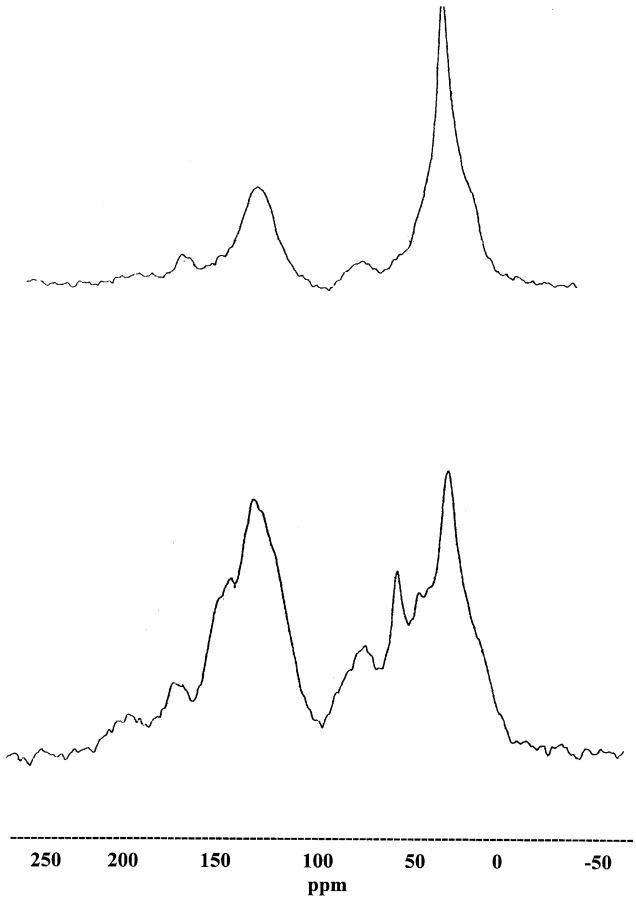

Fig. 2. ^{13}C CPMAS NMR spectra of sapropels 376/2-2 (top) and 378/1-1 (bottom).

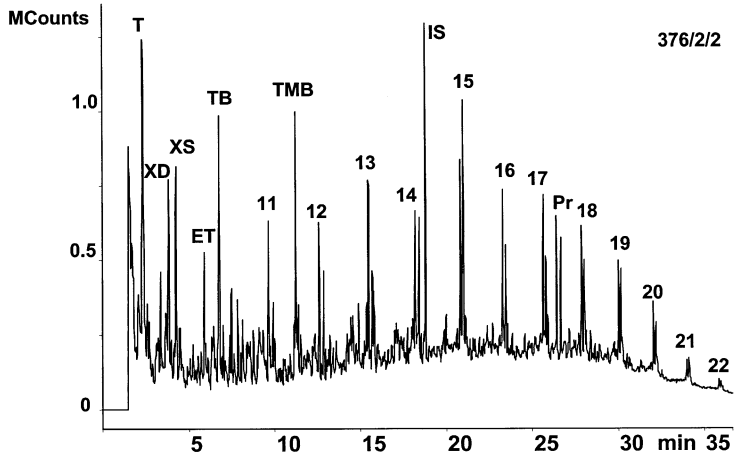

Fig. 3. Reconstructed ion chromatogram obtained from the pyrolysis of 5.4 mg of sapropel 376/2-2. T: toluene; XD: *m*/*p* xylene + 2,5-dimethylthiophene; XS: *o*-xylene + styrene; ET: ethylmethylthiophene = C33 benzene; TB: 1,2,4-trimethylbenzene; TMB: 1,2,3,4-tetramethylbenzene; IS: internal standard; and numbers 11–21: carbon numbers of *n*-alkane/*n*-alk-1-ene doublets.

Given correct assignments of the chemical shifts of each NMR absorption, it is straightforward to estimate the elemental H/C and O/C ratios of the organic material comprising the sapropels. Such estimates are included in Table 2. The greatest uncertainties in these elemental ratios derive from the poor resolution of the aliphatic carbons between 15 and 45 ppm (most of which have been assigned to methylene groups) and from the difficulties in distinguishing between carbon atoms in alcohols and ethers within the range of chemical shifts between 85 and 55 ppm. The values of these estimated H/C ratios are reasonably close to the values obtained by direct measurement (Table 2). The direct measurements are less accurate than one would wish, since the eastern Mediterranean sapropels contain between only 2 and 20% of organic carbon and considerable demineralisation of the samples was necessary before they could be combusted reliably. Table 2 shows that, because of its increased aromaticity, sapropel 378/1-1 possessed a significantly lower elemental H/C ratio. The H/C ratios of the other eastern Mediterranean sapropels were similar both to the H/C ratios of the Black Sea sapropels studied previously and to a Type I kerogen oil-shale [13], but greater than the elemental ratios displayed by Type II oil-shales [14]. The elemental O/C ratios estimated from the NMR spectra were significantly larger than those observed in either Black Sea sapropels or the samples of Types I and II kerogen oil-shales we have examined. The ratios are consistent with both the discussion of the infra-red spectra and the results of previous workers [12,23–29] in indicating the sapropels to have experienced oxidation, since their deposition.

The aromaticities of the eastern Mediterranean sapropels were generally similar to those of the Black Sea sapropels and also to the Type I kerogen oil-shale [13]. The degree of alkyl substitution of the aromatic rings in the eastern Mediterranean sapropels, however, was generally similar to that in the Type II kerogen oil-shales rather than to the Type I oil-shale. The Pleistocene sample, 378/1-1, from the Cretan basin was exceptional in possessing an aromaticity similar to that of the immature Type II oil-shales [14]

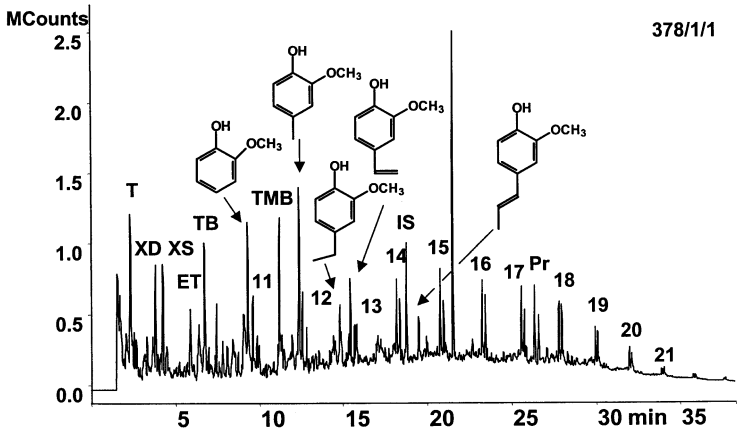

Fig. 4. Reconstructed ion chromatogram obtained from the pyrolysis of 5.4 mg of sapropel 378/1-1. Abbreviations as for Fig. 3.

and having aromatic rings, which were more highly substituted by oxygen atoms than any of the other samples examined.

Table 2 shows the average alkyl chain length of the eastern Mediterranean sapropels to be significantly shorter than the chain lengths of either the Black Sea sapropels or the Type I kerogen oil-shale and to lie in the range observed in the Type II kerogen oil-shales. (The latter observation may be incorrect, since the higher O/C ratios observed in the eastern Mediterranean sapropels were partly due to the number of aliphatic carboxyl groups observed in both the NMR and the infra-red spectra and were these carboxyl groups included as terminators of chains—in addition to the methyl groups—the average chain lengths of the sapropels would have been even smaller.) The infra-red and NMR estimates of relative chain length included in Table 2 vary similarly between samples. However, the infra-red estimates, being ratios of the absorption due to the asymmetric C–H vibrations of methylene and methyl groups, incorporate extinction coefficients. The NMR estimates being a factor of 1.4–2.4 larger than the infra-red estimates, it appears that the extinction coefficient for the asymmetric vibration of methylene groups was about half that for the asymmetric vibrations of methyl groups. This is consistent with compilations of infra-red spectra [39], which indicate the absorptions due to the asymmetric stretching of methylene and methyl groups to be approximately equal in *n*-heptane suggesting the ratio of the corresponding extinction coefficients to be 0.6–0.7.

3.3. Py-GC/MS

3.3.1. Introduction

Pyrograms obtained from samples 376/2-2 and 378/1-1 are displayed in Figs. 3 and 4. Whereas the pyrogram from 378/1-1 will be shown to be unique, pyrograms from all the other samples were remarkably similar and that obtained from sample 376/2-2 may be accepted as typical.

Table 3 lists those products which gave significant distinguishable peaks, which could tentatively be identified from their corresponding mass spectra. These compounds occurred in the first 2000 scans of the mass range covered by the spectrometer and accounted for between 5 and 10% of the total organic matter in each sapropel. From these compounds, 46 exemplars were selected for quantitative estimation and grouped into nine classes suggested both by the chemistry of the compounds in Table 3 and by previous studies of sapropels to which reference will be made in the ensuing discussion. These 46 compounds are listed in Table 4, which compares the relative areas of each of the nine component classes.

Table 4 reveals that only sample 378/1-1 generated a significant proportion of guaiacols (2-methoxyphenols, mainly 4-alkylated-2-methoxyphenols); syringols (2:6-dimethoxyphenols) and vinyl phenol were present only in very low concentrations. Thus, consistent with the relatively high aromaticity shown by its NMR spectrum, 378/1-1 contained much aromatic material derived from lignin, probably from deciduous soft-wood. The identification of guaiacols and the comparative absence of syringols was confirmed by repeating the pyrolysis in the presence of tetramethyl ammonium hydroxide (thermochemolysis), when methylated benzene carboxylic acid derivatives of guaiacols were generated. The principal benzene carboxylic acid was the methyl ester of 3,4-dimethoxy-benzoic acid, whose presence has been suggested [40] to indicate microbial attack on the lignin polymer. It seems clear that the Pleistocene sapropel, 378/1-1, deposited in the Cretan basin close to small fertile islands, alone of the eastern Mediterranean sapropels we have examined, derived to a significant extent from lignin.

3.3.2. Alkyl aromatics

Table 4 shows between about 40 and 70% of the area of the pyrograms to have been comprised of alkyl aromatics, in this sense the most common class of compound generated from the eastern Mediterranean sapropels. Indeed, the most common individual compound in the pyrograms was toluene, whose presence accounted for between 0.5 and 1.5 parts per thousand of the total organic carbon in the sapropels. Given that, save for 378/1-1, none of the eastern Mediterranean sapropels were derived from lignin it is tempting to consider toluene being generated by the diagenesis or the pyrolysis of phenylalanine structures in proteins. Products characteristic of proteins, such as indoles and aromatic nitriles could not be observed in larger than trace quantities from the pyrolysis of the eastern Mediterranean sapropels and if toluene derived from phenylalanine structures, these structures must have been selectively preserved during diagenesis. We therefore suggest toluene to have been formed by the pyrolysis of humic acids. Humic acids have different structures depending on whether they are formed from the diagenesis of terrigeneous, lignin containing, or from marine organic material [41,42], but they appear to possess major structures in common and humic acids from both terrigeneous and marine depositions, when pyrolysed under the conditions employed here generated toluene in larger quantities than any other compound [42].

The aromatic compounds generated by pyrolysis of the eastern Mediterranean sapropels and compiled in Table 4 included, besides benzene and toluene, alkyl benzenes, indenes and alkylated naphthalenes. Save for sapropel 376/6-4, pyrolysis of each sapropel gave a distribution of alkyl benzenes similar to that shown in Fig. 5. This was even true of sapropel 378/1-1, which gave the smallest yield of alkyl aromatics. It seems clear that, whereas about half of the aromatic material in this sapropel derived from lignin, the alkyl benzenes were generated from different structures

Table 3
Identification of the major products from flash pyrolysis (250 μg of 1,3,5-tri, *tert*-butylbenzene were generally used as an internal standard)

Compound	Key reference ions (*m*/*z*)	Compound	Key reference ions (*m*/*z*)
Benzene	78	Methylcyclohexadiene	79, 94
Toluene	91, 92	2-Methylthiophene	97, 98
3-Methylthiophene	97, 98	2-Methylpyrrole	80, 81
3-Methylpyrrole	80, 81	Ethylbenzene	91, 106
2-Ethylthiophene	97, 102	2,5-Dimethylthiophene	111, 112
m/*p* Xylene	91, 106	2,4-Dimethylthiophene	111, 112
2,3-Dimethylthiophene	111, 112	Styrene	104
Benzenethiol	110	*o*-Xylene	91, 106
n-Non-1-ene	55	*n*-Nonane	57
2-Cyclopenten-1-one	67, 96	4-Ethylphenol	105, 107
Dimethylpyrrole	94, 95	Propylbenzene	91, 120
2-Propylthiophene	97, 126	2-Ethyl-5-methylthiophene	111, 126
Phenol	94	2,3,4-Trimethylthiophene	111, 126
4-Methyl benzenetriol	123, 124	1,2,4-Trimethylbenzene	105, 120
n-Dec-1-ene	55	*n*-Decane	57
4-Ethyl-2-methylpyrrole	94, 109	2,3,4-Trimethylpyrrole	108, 109
1,2,3-Trimethylbenzene	105, 120	4-Ethyl-3-methylpyrrole	94, 109
2,3-Dimethylcyclopent-2-en-1-one	67, 110	3-Ethyl-4-methylpyrrole	94, 109
Indene	115, 116	2-Methyl-5-propylthiophene	111, 140
o-Methylphenol	107, 108	*n*-Butylbenzene	92, 134
Phenylpropanone	105, 134	C_4 Thiophene	125, 140
m/*p* Methylphenol	107, 108	2-Methoxyphenol (guaiacol)	109, 124
2,3-Dimethyl-4-ethylpyrrole	108, 123	*n*-Dec-1-ene	55
2,4-Dimethyl-3-ethylpyrrole	108, 123	*n*-Undecane	57
3-Phenyl-2-propenal	131, 132	3,5,5-Trimethylcyclohex-2-ene-1-one	82, 138
2,3,4,5-Tetramethylpyrrole	122, 123	Dihydromethylnaphthalene	129, 124
Methylindene	115, 130	1,2,3,4-Tetramethylbenzene	119, 134
2-Pentylthiophene	111, 154	*n*-Pentylbenzene	92, 146
Naphthalene	128	3-Ethyl-2,4,5-trimethylpyrrole	122, 137
Benzothiophene	89, 134	Methylguaiacol	123, 138
n-Dodec-1-ene	55	Trimethylphenol	212, 236
n-Dodecane	57	2-Methyl-3-phenylpropanal	145, 146
n-Hexylthiophene	111, 168	*n*-Hexylbenzene	91, 162
Ethylguaiacol	137, 152	2-Methylnaphthalene	141, 142
Methylbenzothiophene	147, 148	*n*-Tridec-1-ene	55
n-Tridecane	57	1-Methylnaphthalene	141, 142
Vinylguaiacol	135, 150	Trimethyltetrahydronaphthalene	159, 174
n-Heptylthiophene	111, 182	*n*-Heptylbenzene	91, 176
1,4 Bis {1-Methylethenylbenzene} methylnaphthol?	143, 158	*n*-Tetradec-1-ene	55
n-Tetradecane	57	Dimethylbenzothiophene	161, 162
Trimethylnaphthalene	141, 156	Eugenol	164
n-Octylthiophene	111, 196	*n*-Octylbenzene	91, 190
n-Pentadec-1-ene	55	*n*-Pentadecane	57
Trimethylnaphthalene	155, 170	*n*-Nonylthiophene	111, 210
n-Nonylbenzene	91, 204	*n*-Hexadec-1-ene	55
n-Hexadecane	57	*n*-Decylthiophene	111, 224
n-Decylbenzene	91, 218	*n*-Heptadec-1-ene	55
n-Heptadecane	57	Prist-1-ene	67, 266
Prist-2-ene	67, 266	*n*-Undecylthiophene	111, 238
n-Undecylbenzene	91, 232	*n*-Octadec-1-ene	55
6,10,14-Trimethyl-2-pentadecenone?	58, 25	*n*-Octadecane	57
n-Nonadec-1-ene	55	*n*-Nonadecane	57

Table 4
Percentage areas of pyrograms due to compound classes observed in Py-GC/MS
(This table has been deduced from the quantification of the following compounds) (*n*-alkanes: *n*-decane to *n*-hexadecane; *n*-alkenes: *n*-dec-1-ene to *n*-hexadec-1-ene; Aromatics: benzene, toluene, *m*-xylene, *p*-xylene, *o*-xylene, styrene, 1,2,4-trimethylbenzene, 1,2,3-trimethylbenzene, indene, naphthalene, 1-methyl naphthalene, 2-methylnaphthalene, 1,2,3,4-tetramethylbenzene; Thiophenes: 2-methylthiophene, 2,5-dimethylthiophene, 2-ethyl-5-methylthiophene, 2,3,4-trimethylthiophene; Pyrroles: 3-methylpyrrole, 3-ethyl-4-methylpyrrole, 2,3,5-trimethylpyrrole, 2,4-dimethyl-3-ethylpyrrole; Phenols: phenol, 2-methylphenol, 4-methylphenol, 3-methylphenol; Guaiacols: 2-methoxyphenol (guaiacol), 4-methyl-2-methoxyphenol, 4-ethyl-2-methoxyphenol; Pristenes: prist-1-ene, prist-2-ene; Cyclic ketones: methylcyclopentenone; trimethylcyclohexenone)

Sapropel	374/5-3	375/4-4	376/1-4	376/2-2	376/5-2	376/6-4	377/1-2	378/1-1	378/6-3	378/11-2
n-Alkanes	15.9	9.4	11.1	12.6	11.9	6.1	15.6	8.8	13.2	12.8
n-Alkenes	16.2	9.9	12.0	13.6	10.6	7.1	15.3	10.4	12.8	10.7
Aromatics	47.6	44.1	53.7	50.4	60.0	69.2	47.2	38.3	51.7	54.8
Thiophenes	9.3	28.0	11.2	11.2	10.1	7.6	14.3	7.4	10.0	10.0
Pyrroles	4.5	3.4	5.0	4.4	0.8	1.8	2.1	2.4	4.6	4.4
Phenols	3.4	2.5	3.9	4.6	3.3	4.6	2.4	10.2	3.7	3.6
Guaiacols	–	–	–	0.2	–	0.3	–	19.8	0.2	0.2
Pristenes	1.3	1.5	1.5	1.5	1.1	0.6	1.5	1.1	1.3	1.4
Cyclic-ketones	1.7	1.6	1.9	1.6	2.5	2.5	1.4	1.5	1.9	1.9

common to the other sapropels. Hartgers et al. [43], in considering the formation of alkyl benzenes by the flash pyrolysis of kerogens supposed

(a) each polyalkyl benzene was initially released as a substituted benzyl radical by the scission of an aliphatic carbon–carbon bond β to the benzene ring,

(b) the substituents around this benzene ring were otherwise unchanged by the pyrolysis, even in stereo chemistry. Consequently, each alkylbenzene could be accepted as a biomarker characteristic of specific organic material existing with identical stereochemistry in the parent kerogen, and

(c) toluene and xylenes were formed by aromatisation

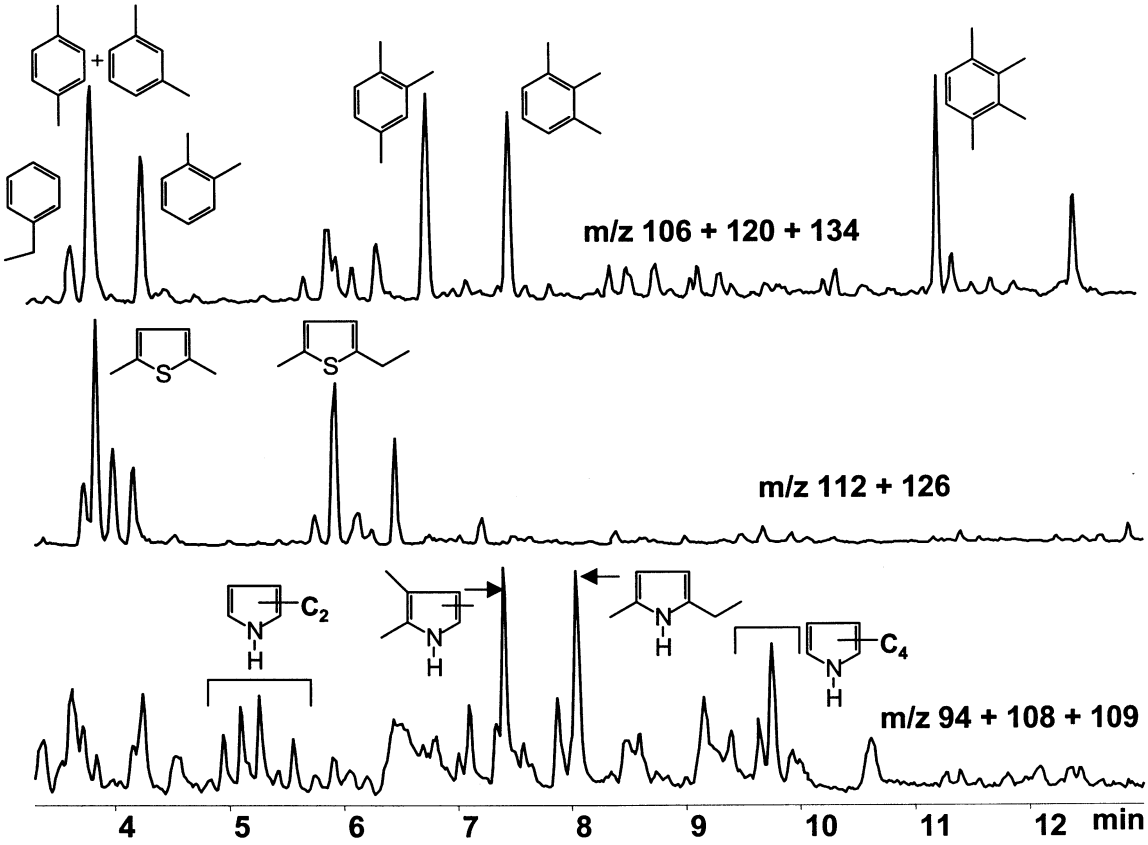

Fig. 5. Mass chromatograms obtained from the pyrolysis of sapropel 375/4-4. Distribution of C_2, C_3 and C_4 alkyl benzenes (top), C_2 and C_3 alkyl thiophenes (middle), and C_2, C_3 and C_4 alkyl pyrroles (bottom).

during the pyrolysis of polymethylene material and of carotenoids present in the kerogen.

Fig. 4 shows the prevalence of meta- and para-xylenes (which co-eluted), 1,2,3- and 1,2,4-trimethylbenzenes and 1,2,3,4-tetramethylbenzenes amongst the compounds generated by the pyrolysis of the sapropels. Hartgers et al. [35,43] observed these structures to be generated from Types II and IIS kerogens; they attributed the xylenes and 1,2,3-trimethylbenzene to aromatisation occurring during the pyrolysis of non-aromatic carotenoids, 1,2,4-trimethylbenzene to the pyrolysis of plastoquinones and 1,2,3,4-tetramethylbenzene (when, as here, accompanied by 1-ethyl, 2,3,6-trimethylbenzene) to the pyrolysis of photosynthetic sulphur bacteria. The relatively high levels of 1,2,3,4-tetramethylbenzene, which have been observed, as well as its origin from photobacteria could be in accordance with the recent identification of isorenieratene derivatives in eastern Mediterranean sapropels [36]. Pyrolysis of sapropel 376/4-4 gave ortho-, rather than meta- and para-xylene, which might suggest the presence of algaenans from microalgae observed in Type I kerogens [43], but no ester linkages, typical of algaenans, were observed in the infra-red spectra (Section 3.1).

Future study of the mechanisms of diagenesis and of the flash pyrolysis of model compounds will doubtless refine suppositions (a), (b) and (c) and improve the attribution of alkyl benzenes. Supposition (c) seems in particular need of clarification. Thus, we observe that, whereas pyrolysis of α carotene under the conditions used here did generate small concentrations of toluene and xylenes (and a substituted cyclopentene, C_9H_{16}), the dominant product was a substituted tetralin, $C_{13}H_{18}$—not generated from the eastern Mediterranean sapropels—and small concentrations of other substituted tetralins and naphthalenes were also observed. Again, clay minerals present in kerogen may be expected to modify the mechanisms of pyrolysis [42].

3.3.3. Alkyl thiophenes

Table 4 shows alkyl thiophenes to have been important products of the pyrolysis of the sapropels, 2-methylthiophene being by far the most abundant. The oldest, Miocene sapropel, 375/4-4, generated the largest yields. Similar, relatively simple distributions of C_2 and C_3 thiophenes were observed from all sapropels (Fig. 5). Benzothiophene and benzene thiol were also observed. The observations of alkyl thiophenes are consistent with anoxic depositions of all the sapropels. Organic sulphur compounds are formed in recent sediments when the interaction of organic material with inorganic sulphur nucleophiles produced as a result of bacterial reduction of sulphate diminishes concentrations of reactive iron [44,45]. The sulphur nucleophiles appear to add to olefines to form thiols or polysulphides, which may cyclise to form thiolanes or form intermolecular bridges. Further diagenesis yields thiophenes [46–51]. Few sulphur compounds other than thiophenes were observed from the pyrolysis, even of the younger sapropels, and it appears that if such compounds as organic sulphides were present pyrolysis generated either hydrogen sulphide or some, at least, of the observed alkyl thiophenes [1,48,51,52]. If one excludes sapropel 378/1-1, which, unlike the other sapropels, originated from the deposition of terrigeneous material, Table 4 suggests that the concentrations of alkyl thiophenes may have been inversely correlated with the concentrations of alkyl aromatics. Should further studies confirm the inverse correlation, it would be consistent with there being competition between aromatisation and sulphurisation (vulcanisation?) of the organic material either during diagenesis or during pyrolysis.

3.3.4. Pyrroles

Whereas nitrogen-containing biomarkers of proteins and aminoacids were not observed, alkyl pyrroles were formed by the flash pyrolysis of all the sapropels (Table 4). Typical distributions of C_2-, C_3- and C_4-pyrroles are included in Fig. 5. These alkyl pyrroles have been shown to be pyrolysis products of tetrapyrroles [53] and as such are biomarkers of photopigments from vegetation or bacteria.

3.3.5. Alkanes and alkenes

A series of doublets consisting of *n*-alkanes and *n*-alk-1-enes was observed amongst the pyrolysis products of each sapropel (Fig. 3). The series extended from C_8 to about C_{23}, the most intense peaks in the pyrogram being observed between C_{10} and C_{18}. There was little difference between the relative intensities of peaks corresponding to alkanes with odd and even numbers of carbon atoms. The alkanes and alkenes had similar intensities, though, as the chain length increased alkanes became rather more intense than alkenes. Pristenes were the most abundant branched hydrocarbons generated by pyrolysis (Table 4). When sapropel 378/1-1 was pyrolysed in the presence of tetramethyl ammonium hydroxide (thermochemolysis) methyl esters of fatty acids, FAMES, notably the *n*-C_{12}, *n*-C_{14} and *n*-C_{16} fatty acids were observed by subsequent GC/MS analysis. Whereas carboxylic acids were readily observed in the ^{13}CPMAS NMR spectra (Fig. 2 and Section 3.2), neither carboxylic acids nor FAMES appeared significant in any of the pyrograms obtained from the Mediterranean sapropels and it must be supposed that pyrolysis of the carboxylic acids generated alkanes and alkenes.

3.3.6. General

In Table 4, sapropel 378/1-1 stands out by virtue of the high content of guaiacols and phenols and the relatively low content of alkyl benzenes in its pyrolysis products; the other sapropels generally gave similar distributions of products on pyrolysis. From Table 4, one may define an average eastern Mediterranean sapropel as giving on Py-GC/MS, a pyrogram consisting of 11.4 ± 0.6% *n*-alkanes, 11.9 ± 0.7% *n*-alkenes, 49.0 ± 1.4% aromatics, 9.6 ± 0.5% thiophenes, about 4.4% of pyrroles, 3.6 ± 0.25% of phenols, no guaiacols,

$1.35 \pm 0.05\%$ of pristenes and $1.69 \pm 0.07\%$ of cyclic ketones (the percentages of thiophenes and pyrroles in Table 4 are not distributed normally about the mean). Comparison with this standard average sapropel enables one to distinguish.

First, sapropel 376/6-4, whose pyrolysis generated significantly high proportions of aromatics and cyclic ketones and significantly low proportions of *n*-alkanes, *n*-alkenes and pristenes (and abnormal yields of pyrroles). It appears that the deposition of this sapropel was unusual.

Second, the oldest, Miocene sapropel, 375/4-4, which gave a similar distribution of products to the other sapropels, even the youngest, nevertheless differed in yielding a significantly higher proportion of thiophenes. The observed ratio of 2-methylthiophene to toluene generated by pyrolysis was also significantly high and one concludes that sapropel 375/4-4 possessed abnormally high concentrations of organic sulphur.

Third, sapropels 374/5-3 and 377/1-2, from the Ionian basin, which differed from the others in generating significantly higher yields of alkanes and alkenes. Diatoms appeared to be absent from these sapropels [6] and, in view of the importance recently ascribed to diatoms in the deposition of Mediterranean sapropels [18–20], one speculates that the high yield of alkanes was due to the pyrolysis of biopolymers absent from diatoms, but present in the microalgae in the Ionean sapropels [54].

3.4. Hy-Py

3.4.1. Introduction

Previous studies have shown Hy-Py of kerogens to generate larger yields of volatile compounds than flash pyrolysis and, moreover, to accomplish this gently in that the stereochemistry of the products was the same as that of the structures from which they were evolved [14,37]. Hy-Py has therefore been used to compare the detailed aliphatic structures present in sapropel 376/2-2, typical of those eastern Mediterranean sapropels having a marine deposition, and in 378/1-1, whose deposition included much terrigeneous lignin.

3.4.2. Alkanes

Fig. 6 shows the distribution of the *n*-alkanes observed as the major components of gas chromatograms of the aliphatic material separated from the volatiles generated by Hy-Py of sapropels 376/2-2 and 378/1-1. The identity of the *n*-alkanes was confirmed by mass spectrometry. The gas chromatograms from both sapropels extended as far as *n*-C_{36} or *n*-C_{38}. Thus, the sapropels, like the kerogens, generated *n*-C_{11} to *n*-C_{17} alkanes, typical biomarkers of phytoplankton lipids, together with *n*-C_{23} and longer chain material indicative of the presence of higher plants, both terrigeneous and marine [14,55]. Fig. 6 shows the relative concentrations of chains longer than *n*-C_{23} to be higher than the relative concentrations observed previously from kerogens K1 and K2. Gas chromatograms (not shown) of aliphatic material separated from bitumens possessed major humps of unresolved material not observed in the gas chromatograms of the Hy-Py products shown in Fig. 6. The gas chromatograms indicated the bitumens to contain smaller proportions of longer chain alkanes than the parent sapropels.

The chain lengths of the *n*-alkanes generated by the Hy-Py experiments were significantly longer than the chain lengths evolved from flash pyrolysis. Flash pyrolysis furnished few alkanes longer than *n*-C_{23} (Fig. 3). As one would expect, flash pyrolysis cracks longer chain material and one should be cautious in using distributions of *n*-alkanes observed by Py-GC/MS to characterise the deposition of kerogens.

Table 2 includes estimates of the ratios of methylene and methine groups to terminal methyl groups. Doubling of these ratios gives the approximate chain length should Hy-Py convert all the aliphatic material into alkanes. Both the sapropels examined, as well as the Type II kerogen K2, had significantly smaller ratios of methylenes and methines to terminal methyl groups than is indicated by the chain lengths of the alkanes shown in Fig. 6. Only the Type I kerogen, K1, gave similar average chain lengths in the ^{13}C CPMAS NMR and Hy-Py experiments (Table 2 suggests that had the Miocene sapropel, 375/4-4, been subjected to Hy-Py it, too, might have generated a distribution of normal alkanes with a chain length consistent with the NMR results). The lower ratios chain lengths indicated by NMR would be consistent with the presence of branched aliphatics and of aromatic compounds substituted by relatively short alkyl chains which were either removed as gas during the Hy-Py experiments or else contributed to the aromatic products.

3.4.3. Hopanes

Hopanes, presumed to derive from the cell membranes of bacteria [56,57], though present in trivial concentrations which made little contribution to the overall structure of the sapropels, were nevertheless distinguishable in the aliphatics separated after the Hy-Py experiments. Previous work has demonstrated that Hy-Py experiments affect neither the configuration nor the stereochemistry of the hopanes which are released [14,37,58]. Bacteria reproduce and adapt to their environment rapidly but the marked similarity of the hopane distributions in the sapropels 376/2-2 and 378/1-1 shown in Fig. 7 indicates that any adaptation of the bacteria to the different environments of the respective sapropel depositions caused no observable change to the components of their cell membranes though such changes could have subsequently been masked by their binding and diagenesis in the sapropel matrix.

The hopane distributions in sapropels 376/2-2 and 378/1-1 shown in Fig. 7 are compared in Table 5 with hopane distributions in the Types I and II kerogens K1 and K2, and with a recent anoxic sediment. Whereas, the relative concentrations of hopanes from C_{29} to C_{35} in the

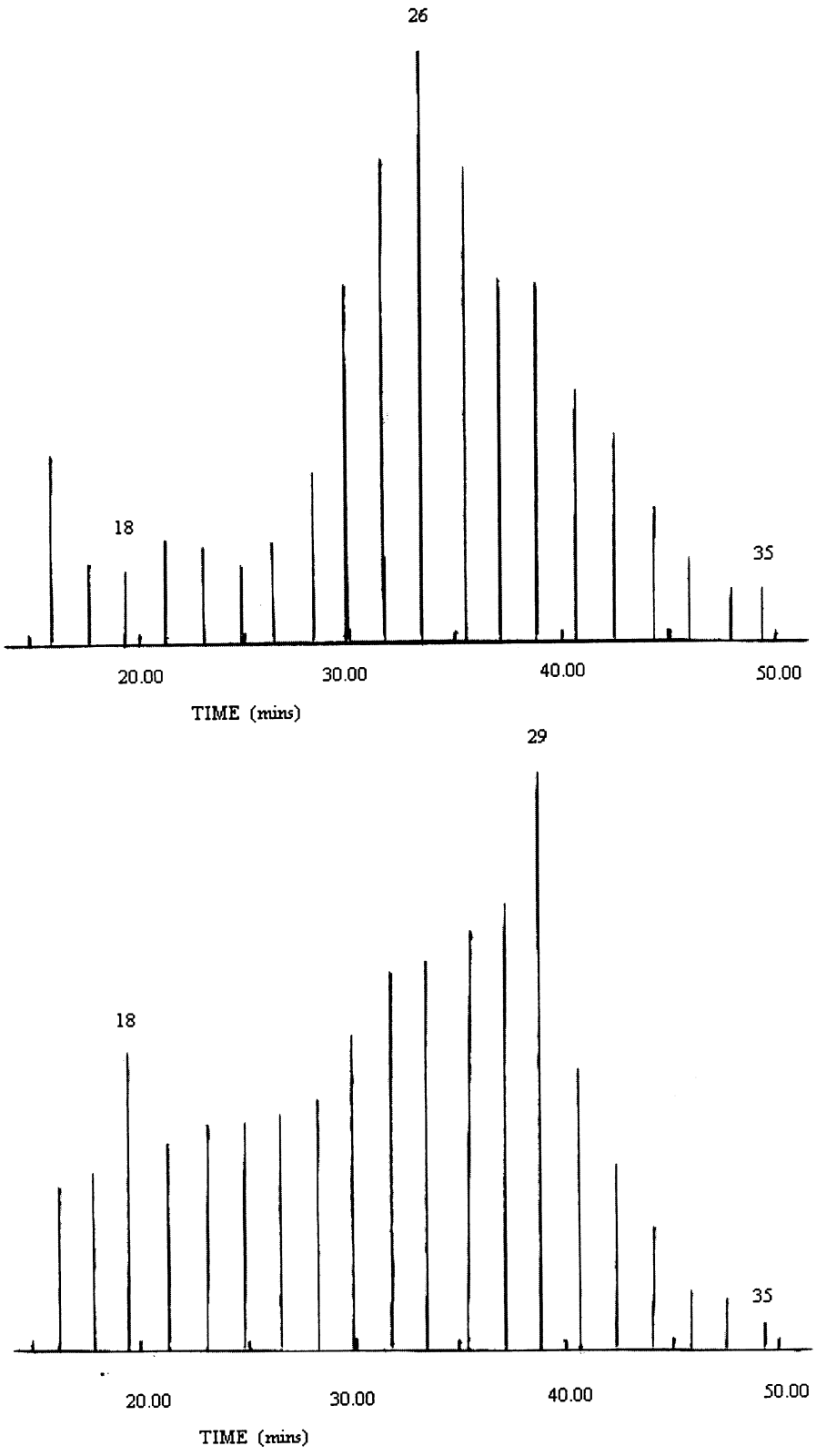

Fig. 6. Reconstructed ion ($m/z = 85$) chromatograms showing the relative intensities and retention times of *n*-alkanes of the aliphatic products generated in Hy-Py experiments on sapropels 376/2-2 (top) and 378/1-1 (bottom). Numbers on the chromatograms indicate the carbon numbers of the *n*-alkanes.

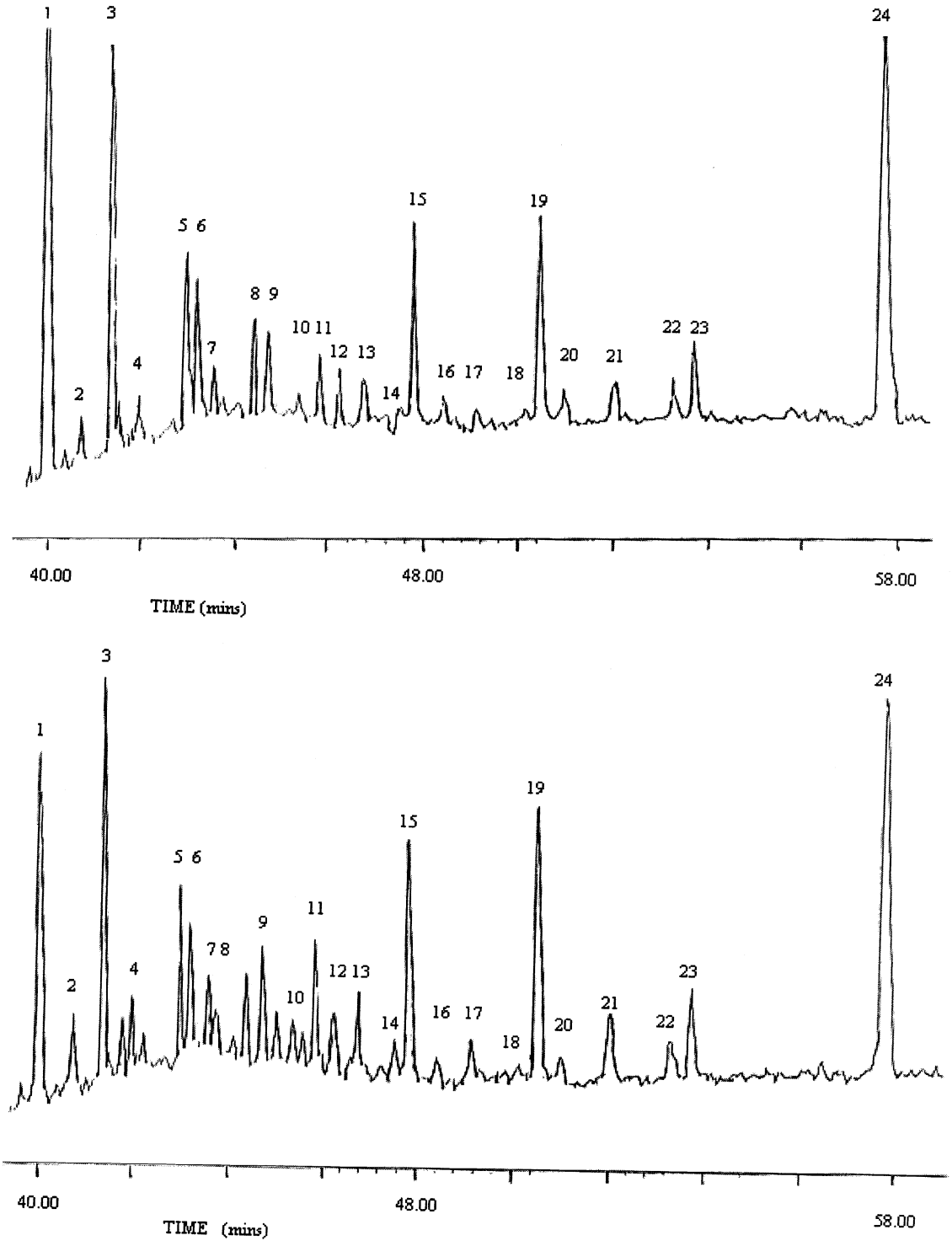

Fig. 7. Ion ($m/z = 191$) chromatograms showing the distribution and retention times of hopanes in the aliphatic products generated in Hy-Py experiments on sapropels 376/2-2 (top) and 378/1-1 (bottom). Key: 1 = 29$\alpha\beta$; 2 = 29$\beta\alpha$; 3 = 30$\alpha\beta$; 4 = 30$\beta\alpha$; 5 = 31$\alpha\beta S$; 6 = 31$\alpha\beta R$; 7 = 30$\beta\beta$; 8 = 32$\alpha\beta S$; 9 = 32$\alpha\beta R$; 10 = 32$\beta\alpha$; 11 = 31$\beta\beta$; 12 = 33$\alpha\beta S$; 13 = 33$\alpha\beta R$; 14 = 33$\beta\alpha$; 15 = 32$\beta\beta$; 16 = 34$\alpha\beta S$; 17 = 34$\alpha\beta R$; 18 = 34$\beta\alpha$; 19 = 33$\beta\beta$; 20 = 35$\alpha\beta S$; 21 = 35$\alpha\beta R$; 22 = 35$\beta\alpha$; 23 = 34$\beta\beta$ and 24 = 35$\beta\beta$. Numbers are carbon numbers of the (pentacyclic triterpane) hopanes; α, β, R and S are conventional symbols indicating chirality.

Table 5
Comparison of hopane distributions

Carbon number	C_{29}	C_{30}	C_{31}	C_{32}	C_{33}	C_{34}	C_{35}
Relative concentrations[a]							
Sapropel 376/2-2	1.24	1.18	0.46	0.51	0.52	0.24	1.0
Sapropel 378/1-1	0.98	1.12	0.47	0.59	0.75	0.27	1.0
K1 [54]	11	5	4.5	2.3	1	0.9	1.0
K2 [55]	8–9	6–8.5	3.5–4.5	3.5	1.7–2.4	1.3	1.0
Recent anoxic sediment[b]	1.0	1.65	1.0	1.4	0.72	0.32	1.0
$\beta\beta$/(all isomers)							
Sapropel 376/2-2	~ 0.05	< 0.05	0.15	0.45	0.5	0.5	0.75
Sapropel 378/1-1	0.1	0.15	0.25	0.4	0.55	0.5	0.8
Recent anoxic sapropel[b]	0.2	0.6	0.65	0.55	0.55	0.5	0.7
$22S/(22S + 22R)$							
Sapropel 376/2-2			0.55	0.55	0.55	0.55	0.45
Sapropel 378/1-1			0.6	0.45	0.45	0.4	0.33
K2 [55]			0.4–0.6	0.3–0.7			0.3–0.7
Recent anoxic sediment[b]			0.4	0.2	0.35	0.4	0.35

[a] All values have been estimated from the relative peak heights of mass spectrometric single ion fragmentograms ($m/z = 191$) of the aliphatic products separated from Hy-Py experiments.
[b] P.Pot anoxic (18–19 cm).

Types I and II kerogens were consistent with an oxic deposition, the significant concentrations of C_{33}, C_{34} and C_{35} hopanes observed both in the recent sediment and in the sapropels indicated their anoxic deposition [56,57,59,60]. In these longer hopanes, those isomers with a $\beta\beta$ configuration clearly dominated those with $\alpha\beta$ and $\beta\alpha$ configurations. The dominance of the less thermodynamically stable $\beta\beta$ configuration observed in bacteria is usually accepted as evidence of geological immaturity [60]. This is clearly consistent with the hopane distributions observed after Hy-Py hydrogenation of the recent sediment (Table 5), where only the C_{29} hopane possessed significant proportions of the $\alpha\beta$ isomer. However, whereas their C_{33}, C_{34} and C_{35} $\beta\beta$ configurations are consistent with the immaturity of the sapropels, the sapropel hopanes C_{29}–C_{32} were dominated, like the hopanes in kerogen K2 by their $\alpha\beta$ isomers, signs of relative maturity. *R*/*S* epimerisation at the C_{22} position is another common indicator of kerogen maturity [60], 22*R* being the less thermodynamically stable epimer, which has been observed in bacteria. The $22S/(22S + 22R)$ ratios shown in Table 5 indicate that the 22*R* epimers in the $\alpha\beta$ isomers in the recent anoxic sediment have yet to achieve thermodynamic equilibrium with the 22*S* epimers, but the epimers in the $\alpha\beta$ isomers from the sapropels were like those in moderately mature Type II kerogens in that thermodynamic equilibrium between the epimers had been established. It is difficult to understand these indicators of maturity in the eastern Mediterranean sapropels and their presence in the trivial quantities of hopane that have been observed could be due to lack of experimental rigour. It will be recalled, however, that infra-red and NMR spectrometry suggest our sapropel samples to have been oxidised and that, after their deposition, Mediterranean sapropels experienced an oxidation front which oxidised their pyrite [23–29]. Oxidation of pyrite is significantly exothermic and, accordingly, it is possible that the passage of the oxidation front through the eastern Mediterranean sapropels acted as catagenesis and produced indications of abnormal maturity by causing degradation and epimerisation of the hopanes. These results should be confirmed by examination of sapropel-containing cores obtained more recently and by comparison of their hopane distributions with their iron and sulphur contents.

3.5. Fluorescence

Table 6 summarises the fluorescence of sapropel 376/2-2, which may be taken as typical of most eastern Mediterranean

Table 6
Summarised fluorescence spectra (B: Bitumen)

Sample	376/2-2	376/2-2B	376/4-4B	378/1-1	378/1-1B
Maximum Fluorescence E_x/E_m (nm)	(265–275)/335 290/350 320/430	270/(360–370) 300/395	268/325 268/365 305/335 305/365 320/365	260/345 320/400	266/330 266/390

sapropels, and sapropel 378/1-1, unique in being formed from terrestrial vegetation, as well as their corresponding bitumens. The sapropels, studied as finely divided suspensions in distilled water, gave broad and weak spectra together with sharp peaks due to the Raman scattering of water; the spectra of the bitumens, studied as dilute solutions in dichloromethane, were more intense. Whereas the fluorescence spectra of the sapropels and their bitumens were different, the wavelengths of their excitation maxima, which never exceeded 320 nm, indicated the aromatic structures in all four samples to be dominated by substituted mono- and di-aromatic rings. The wavelengths of the emission maxima indicate that, although it was mono- and di-aromatic structures, which were excited, energy transfer ensured fluorescence was emitted by polyaromatic nuclei or by excimers and exciplexes. Evidently, the previous discussion of the substitution of the aromatic rings shown by the NMR spectra and based on the sole presence of mono-aromatic structures (Table 2) was too simple.

4. General discussion

4.1. The average sapropel

The complementary results of infra-red and ^{13}C CPMAS NMR spectrometry, Py-GC/MS and Hy-Py analysis have provided a reasonably complete description of the organic chemistry of Pleistocene, Pliocene and Miocene sapropels from the eastern Mediterranean. Nine of the 10 sapropels examined possessed similar organic structures consistent with their deposition from a stratified sea.

The average eastern Mediterranean sapropel gave a ^{13}C NMR spectrum dominated by aliphatic absorption, notably by carbon atoms in long chains. The average aromaticity was 0.22, the aromatic carbon atoms being bonded to oxygen, carbon and hydrogen atoms in the ratios 0.89:1.18:3.93. Fluorescence spectroscopy showed the aromatic structures to be dominated by substituted mono- and di-aromatic rings. The NMR spectra indicated elemental H/C and O/C ratios of 1.79 and 0.24, respectively.

On flash pyrolysis such an average sapropel generated a pyrogram, whose area was comprised of $11.4 \pm 0.6\%$ *n*-alkanes, $11.9 \pm 0.75\%$ *n*-alkenes, $49.9 \pm 1.4\%$ alkyl aromatics, $9.6 \pm 0.5\%$ alkyl thiophenes, about 4.4% pyrroles, $3.6 \pm 0.25\%$ phenols, $1.35 \pm 0.05\%$ pristenes, the most abundant branched material, and $1.69 \pm 0.07\%$ of cyclic ketones. Chemothermolysis indicated that many of the alkanes and alkenes were evolved from aliphatic carboxylic acids, shown to be present by the infra-red and NMR spectra of the sapropels.

4.2. Hydrogenation

Consistent with previous work, [14,37,58], catalytic hydrogenation of the sapropels showed the chemical structures generated by their flash pyrolysis to have been constrained by the cracking, which had occurred. In particular, catalytic hydrogenation indicated that, if sapropel 376/2-2 may be taken as typical, the majority of the alkanes generated from the sapropels arose from *multicellular* marine vegetation. Such hydrogenation experiments also indicated marine, as well as terrigeneous plants to have participated in the formation of sapropel 378/1-1. Tiny concentrations of C_{29}–C_{35} hopanoids characteristic of bacteria were also shown by the hydrogenation experiments to have been components of the sapropels.

4.3. The range of variations in structure

As in the Black Sea, [61], the rapid deposition of the original organic particulates in the eastern Mediterranean appears to result in characteristic features of the surface environment being reflected in the organic chemistry of the sea bed and, not surprisingly, some sapropels exhibit significant exceptions to the average analyses. Thus,

- The 10th, Pleistocene sapropel, 378/1-1, deposited in the Cretan basin was singular in possessing a relatively high aromaticity of ~0.4; at least half of its aromatic structure derived from terrigeneous vegetation and accordingly it was the only sapropel to yield guaiacol structures on pyrolysis.
- Sapropel 376/6-4 gave significantly higher proportions of aromatics and cyclic ketones and significantly lower proportions of alkanes, alkenes and pristenes.
- Sapropel 375/4-4 gave higher proportions of thiophenes and a high NMR chain length.
- Sapropels 374/5-3 and 377/1-2 from the Ionian basin gave higher proportions of alkanes and alkenes.

4.4. Oxidation

One must be cautious in relating the observed organic chemistry of the sapropels to their deposition, since both the infra-red and the NMR spectroscopy indicate the sapropels to have become oxidised, probably by an oxidation front which previous workers have observed to remove both pyrite and organic material from eastern Mediterranean sapropels subsequent to their deposition [12,23–29] though it is possible that oxidation occurred during the retrieval or storage of the sapropels.

4.5. Crosslinking in kerogens

A significant gap in this description of the chemistry of the sapropels is the failure to show how the variety of structures revealed by their flash pyrolysis is linked together so that only about 5% of the sapropels was soluble bitumen and 95% was insoluble kerogen. Understanding the linkages implies refining the interpretation of the NMR spectra to yield descriptions of the numbers of the various types of cross-linkages.

4.6. The classification and deposition of the sapropel kerogens

The elemental H/C ratios of the sapropels and the aromaticities derived from their NMR spectra are similar to those observed in Type I kerogens (Table 2), but when the H/C ratios are plotted against the rather high elemental O/C ratios estimated from the NMR spectra, they give a reasonable Type II kerogen plot on a van Krevelen diagram (not shown). The previous paragraph indicated the relatively high oxygen contents could have been due to oxidation, in which case it would be appropriate to regard the eastern Mediterranean sapropels as oxidised Type I kerogens. However, the classification of these sapropels as Type II kerogens would be consistent with the average chain lengths indicated by the NMR spectra and the distribution of C_2–C_4 alkyl benzenes generated by flash pyrolysis. The alkyl thiophenes generated by flash pyrolysis suggest the sapropels might be classified as Type IIS kerogens.

The composition of the hopanes liberated in the Hy-Py experiments is consistent with an anoxic deposition of the sapropels and the dominance of the $\alpha\beta$ isomers in the longer hopanes is consistent with their geological immaturity. The presence of C_{29}, C_{30} and C_{31} hopanes in which $\alpha\beta$ isomers dominated, usually regarded as an indication of geological maturity, is assumed to have been caused by effective catagenesis produced by the exothermic oxidation front supposed to have been experienced by the sapropels after their deposition.

Types I and II kerogens are often associated with lacustrine and marine depositions, respectively. Both the Black Sea sapropels, regarded as Type I kerogens, [1], and the eastern Mediterranean sapropels were deposited from seas which were apparently stratified by the introduction of river water into their surface [1,6]. It is hardly surprising, therefore, that the classification of the eastern Mediterranean sapropels into Types I and II kerogens is uncertain and that comparatively small differences in the depositional environment may have caused sapropels in some basins at certain times to be classified differently to others. Both in the recent geological past and in the present, a major difference between the Black and the eastern Mediterranean seas has been the increased temperature and consequent evaporation which the Mediterranean experienced (notably, of course, during the Messinian salinity crisis). The eastern Mediterranean sapropels would generally have been deposited in a more saline environment than the Black Sea sapropels, consistent with their classification as Types II and I kerogens, respectively.

When the salinity of the Black Sea increased, the deposition of sapropel-varve couples was replaced by the deposition of coccolith-varve couples. The deposition of sapropels from a whole range of phytoplankton species [5] in the more saline Mediterranean suggests the cessation of sapropel formation in the Black Sea to have been due to a decline in the rate of deposition of organic material rather than to the change in the species of the phytoplankton.

4.7. Source rocks

Though few eastern Mediterranean sapropels contain more than 10% of organic carbon [2], they can be considered as precursors of source rocks in the sense that, from the chemistry revealed here, one may readily construe that, with continuing subsidence, increase in temperature will cleave weak bonds and generate molecules—such as the alkanes/alkenes and alkyl aromatics formed by pyrolysis and by hydrogenation in the present investigation—which will be squeezed out as crude oil. How it is that this will be accompanied by an increase in reflectance to 0.5–1.0%, we do not yet understand.

5. Conclusions

The techniques used to describe the structures of Holocene, marinite sapropels essentially Type I kerogens deposited below the Black Sea, [1], have been extended successfully so as to describe the Pleistocene to Miocene eastern Mediterranean sapropels (Types I–II kerogens). Both sets of sapropels have been shown to possess similar organic structures having aromaticities of ~0.2 similar to those of Type I kerogens. Both sets of sapropels are expected to generate source rocks. The major differences between the two sets of sapropels are

- The ratios of methylene plus methine groups to terminal methyl groups (Table 2) in the eastern Mediterranean sapropels are less than a half of those observed in the Black Sea sapropels and the numbers of alkyl substituents on aromatic carbon atoms are twice the numbers found in Black Sea sapropels. In these respects, the eastern Mediterranean sapropels are more similar to Type II than Type I kerogens.
- The eastern Mediterranean sapropels, being formed from the rapid deposition of organic particulates from a range of surface environments, show a wider range of structures than the Black sea sapropels. Thus, the deposition of 378/1-1 contained terrigeneous vegetation and consequently this sapropel had twice the normal aromaticity.
- Oxidation of the eastern Mediterranean sapropels presumably by a front subsequent to their deposition modified their organic structures.

In the present study, not only has the Py-GC/MS technique been improved to provide information about nine classes of compound formed in the flash pyrolysis of the eastern Mediterranean sapropels (Table 4), catalytic hydrogenation of the eastern Mediterranean sapropels has further extended the information obtained by Py-GC/MS by generating both higher molecular weight alkanes originating from multicellular, marine vegetation and cracked during

Py-GC/MS and also stereochemically unchanged hopanes characteristic of bacteria.

Acknowledgements

We are extremely grateful, as indeed we hope are our readers, to the Museums of the Lamont-Doherty Geological Observatory for the gift of the eastern Mediterranean sapropels originally obtained by the careful, innovative work of the DSDP. It was especially kind to have taken so much trouble in the selection of the samples. DF is grateful to the University of Bologna for financial support and GDL thanks the NERC for funding a Post-Doctoral Fellowship.

References

[1] Brown SD, Chiavari G, Ediger V, Fabbri D, Gaines AF, Galletti G, Karayigit AI, Snape CE, Sirkecioglu O, Toprak S. Fuel 2000;34:1725–42.
[2] Hsu KJ, Montadert L, et al. Initial reports of the deep sea drilling project, Vol. 42. Washington, DC: US Government Printing Office, 1978. p. 1–1249.
[3] Kidd RB, Bianca M, Ryan WBF. Reference 1978;2:421–43.
[4] Sigl W, Chamley H, Fabricus F, d'Argand GG, Muller J. In: Initial reports of the deep sea drilling project, Vol. 42. Washington, DC: US Government Printing Office, 1978. p. 445–65.
[5] Kidd RB, Bernoulli D, Garrison RE, Fabricus FH, Melieres F. In: Initial reports of the deep sea drilling project, Vol. 42. Washington, DC: US Government Printing Office, 1978. p. 1079–94.
[6] Cita MB, Grignani D. In: Schlanger SO, Cita MB, editors. Nature and origin of cretaceous carbon-rich facies. London: Academic Press, 1982. p. 165–96.
[7] Hsu KJ, Montadert L, Bernoulli D, Cita MB, Erickson A, Garrison RE, Kidd RB, Melieres F, Muller C, Wright R. In: Initial reports of the deep sea drilling project, Vol. 42. Washington, DC: US Government Printing Office, 1978. p. 1053–78.
[8] Cita MB, Ryan WBF. In: Initial reports of the deep sea drilling project, Vol. 42. Washington, DC: US Government Printing Office, 1978. p. 1405–15.
[9] Wright R. In: Initial reports of the deep sea drilling project, Vol. 42. Washington, DC: US Government Printing Office, 1978. p. 837–46.
[10] Ganssen G, Troelstra SR. Mar Geol 1987;75:221–30.
[11] Sancetta C. Nature 1999;398:27–9.
[12] Rohling EJ, editor. Fifth decade of Mediterranean and sapropel studies, Special issue. Mar Geol 1999;153.
[13] Putun E, Akar A, Ekinci E, Frere B, Bartle KD, Snape CE, Citiroglu M. J Petrol Geol 1991;14:459–64.
[14] Murray I, Love GD, Snape CE, Bailey NJL. Org Geochem 1998;29:981–6.
[15] Diester-Haas L, Robert C, Chamley H. Proceedings of the ocean drilling program: scientific results, Vol. 160. College Station, TX: Texas A and M University, 1998. p. 227–48.
[16] Rossignol-Strick M, Paterne M. In: Rohling, EJ, editor. Fifth decade of Mediterranean and sapropel studies, Special issue. Mar Geol 1999;221–37.
[17] Rossignol-Strick M. Nature 1983;304:46–9.
[18] Kemp AES, Pearce RB, Koizumi I, Pike J, Rance SJ. Nature 1999;398:57–61.
[19] Kemp AES, Pearce RB, Koizumi I, Pike J, Rance SJ. Nature 1999;399:84.
[20] Kemp AES, Pike J, Pearce RB, Lange CB. Deep-Sea Res II 2000;47:2129–54.
[21] Rossignol-Strick M. Palaeogeogr Palaeoclimatol Palaeoecol 1985;49:237–63.
[22] Cheddadi R, Rossignol-Strick M, Fontugne M. Mar Geol 1991;100:53–66.
[23] Pruyers PA, de Lange GJ, Middelburg JJ. Mar Geol 1991;100:137–54.
[24] Higgs NC, Thomson J, Wilson TRS, Croudace IW. Geology 1994;22:423–6.
[25] Thomson J, Higgs NC, Wilson TRS, Croudace IW, de Lange GJ, van Santvoort PJM. Geochim et Cosmochim Acta 1995;59:3487–501.
[26] Van Os B, Middelburg JJ, de Lange GJ. Aquatic Geochem 1996;1:303–12.
[27] Bouloubassi I, Rullkotter J, Meyers PA. In: Rohling, EJ, editor. Fifth decade of Mediterranean and sapropel studies, Special issue. Mar Geol 1999;177–97.
[28] Passier HF, Middelburg JJ, Van Os BJH, de Lange GJ. Geochim Cosmochim Acta 1996;60:751–63.
[29] Passier HF, Bosch H-J, Nijenhuis IA, Lourens LJ, Bottcher ME, Leenders A, Sinninghe Damste JS, de Lange GJ, de Leeuw JW. Nature 1999;397:146–9.
[30] Deroo G, Herbin JP, Roucache J. Reference 1978;2:465–72.
[31] Ten Haven HL, Baas M, de Leeuw JW, Schenck PA. Mar Geol 1987;75:137–56.
[32] Ten Haven HL, Baas M, de Leeuw JW, Schenck PA, Brinkhuis H. Chem Geol 1987;64:149–67.
[33] Ten Haven HL, Baas M, de Leeuw JW, Schenck PA, Ebbing J. Geochim Cosmochim Acta 1987;51:803–10.
[34] Sinninghe-Damste JS, Kock-van Dalen AC, de Leeuw JW, Schenck PA. J Chromatogr 1986:435–52.
[35] Hartgers WA, Sinninghe-Damste JS, de Leeuw JW. J Chromatogr 1992;606:211–20.
[36] Sinninghe-Damste JS, Eglinton TI, de Leeuw JW. Cosmochim Geochim Acta 1992;56:1743–51.
[37] Love GD, Snape CE, Carr AD, Houghton AC. Org Geochem 1995;23:981–6.
[38] Rao CNR. Chemical applications of infrared spectroscopy. New York: Academic Press, 1963.
[39] Simons WW, editor. The Sadtler handbook of infrared spectra. 1978.
[40] del Rio JC, Hatcher PG. Humic and fulvic acids. ACS Symp Ser 1996;651:78–95.
[41] Balkas TI, Basturk O, Gaines A, Salihoglu I. Fuel 1983.
[42] Fabbri D, Mongardi M, Montanari L, Galletti GC, Chiavari G, Scotti R. Fresnius J Anal Chem 1998;362:299–306.
[43] Hartgers WA, Sinninghe-Damste JS, de Leeuw JW. Geochim Cosmochim Acta 1994;58:1759–75.
[44] Sinninghe-Damste JS, de Leeuw JW. Org Geochem 1990;16:1077–101.
[45] Valisolalo J, Perkins N, Chappe B, Albrecht P. Tetrahedron Lett 1984;25:1183–6.
[46] Aizenshat Z, Stoler A, Cohen Y, Nielsen H. Adv Org Geochem 1987;11:563–71.
[47] La Londe RT, Ferrara LM, Hayes MP. Org Geochem 1987;11:563–71.
[48] Sinninghe-Damste JS, Eglinton TI, de Leeuw JW, Schenck PA. Geochim Cosmochim Acta 1989;53:873–89.
[49] Krein EB, Aizenshat Z. J Org Chem 1993;58:6103–8.
[50] Kohnen MEL, Sinninghe-Damste JS, Ten Haven HL, de Leeuw JW. Nature 1989;341:640–1.
[51] Sinninghe-Damste JS, Rijpstra WIC, Kock-van Dalen AC, de Leeuw JW, Schenck PA. Geochim Cosmochim Acta 1989;53:1343–55.
[52] Brown SD, Sirkecioglu O, Snape CE, Eglinton TI. Energy Fuels 1997;11:532–8.
[53] Sinninghe-Damste JS, Eglinton TI, de Leeuw JW. Geochim Cosmochim Acta 1992;56:1743–51.
[54] Gelin F, Volkman JK, Largeau C, Derenne S, Sinninghe-Damste JS, de Leeuw JW. Org Geochem 1995;23:981–6.
[55] Blumer M, Guillard RR, Chase T. Mar Biol 1971;8:183.

[56] Ourisson G, Albrecht PA. Accounts Chem Res 1992;25:398–402.
[57] Ourisson G, Albrecht PA. Accounts Chem Res 1992;25:403–8.
[58] Love GD, Snape CE, Fallick AE. Org Geochem 1998;28:797–811.
[59] Mackenzie AS. In: Brooks J, Welte D, editors. Advances in petroleum geochemistry. New York: Academic Press, 1984. p. 115–214.
[60] Farrimond P, Taylor A, Telnaes N. Org Geochem 1998;29:1181–98.
[61] Ergin M, Gaines A, Galletti GC, Chiavari G, Fabbri D, Yucesoy-Eryilmaz F. Appl Geochem 1996;11:711–20.